ELSEVIER

Tectonophysics 347 (2002) 217–230

TECTONOPHYSICS

www.elsevier.com/locate/tecto

Precursory accelerating seismic crustal deformation in the Northwestern Anatolia Fault Zone

B.C. Papazachos, A.S. Savvaidis, G.F. Karakaisis *, C.B. Papazachos

Geophysical Laboratory, School of Geology, University of Thessaloniki, Thessaloniki 54006, Greece

Received 23 October 2000; accepted 14 January 2002

Abstract

We present the results of a systematic search for the identification of accelerating seismic crustal deformation in the broader northern Aegean area and in northwestern Turkey. We found that accelerating seismic deformation release, expressed by the generation of intermediate magnitude earthquakes, is currently observed in NW Turkey. On the basis of the critical earthquake model and by applying certain constraints which hold between the basic quantities involved in this phenomenon, it can be expected that this accelerating seismic activity may culminate in the generation of two strong earthquakes in this area during the next few years. The estimated epicenter coordinates of the larger of these probably impending earthquakes are 39.7°N–28.8°E, its magnitude is 7.0 and its occurrence time t_c=2003.5. The second strong event is expected to occur at t_c=2002.5 with a magnitude equal to 6.4 and epicenter coordinates 40.0°N–27.4°E. The uncertainties in the calculated focal parameters for these expected events are of the order of 100 km for the epicenter, ±0.5 for their magnitude and ±1.5 years for their occurrence time.

Keywords: Accelerating seismic deformation; Anatolia; Aegean

1. Introduction

The westernmost part of the North Anatolian Fault Zone, which is investigated in the present paper, includes the Marmara Sea area and the northern part of the Aegean Sea (Fig. 1) and is defined by the 38.5°N, 42.0°N parallels and the 24.0°E, 30.0°E meridians. Historical data show that earthquakes with magnitudes up to about 7.5 repeatedly occurred in this area and caused considerable destructions and loss of life (Ambraseys and Finkel, 1995; Papazachos and Papazachou, 1997). During the 20th century only, 15 mainshocks with magnitudes ranging between 6.0 and 7.6 have occurred in this area.

Due to the fact that a large part of this zone is a densely populated area where the Istanbul urban area of more than 10 million people is located and because of the well known westward migration of the seismic activity along the North Anatolian Fault (Allen, 1969; Dewey, 1976; Toksoz et al., 1979; Stein et al., 1997), the generation of the very destructive Izmit earthquake (17.8.1999, *M*=7.6, 40.76°N, 29.97°E) east of Marmara stimulated a series of studies on the future evolution of seismic activity in this region (Parsons et al., 2000; Hubert-Ferrari et al., 2000; Ambraseys and Jackson, 2000; Papadimitriou et al., 2001). In

* Corresponding author.
E-mail address: karakais@geo.auth.gr (G.F. Karakaisis).

0040-1951/02/$ - see front matter © 2002 Elsevier Science B.V. All rights reserved.
PII: S0040-1951(02)00030-6

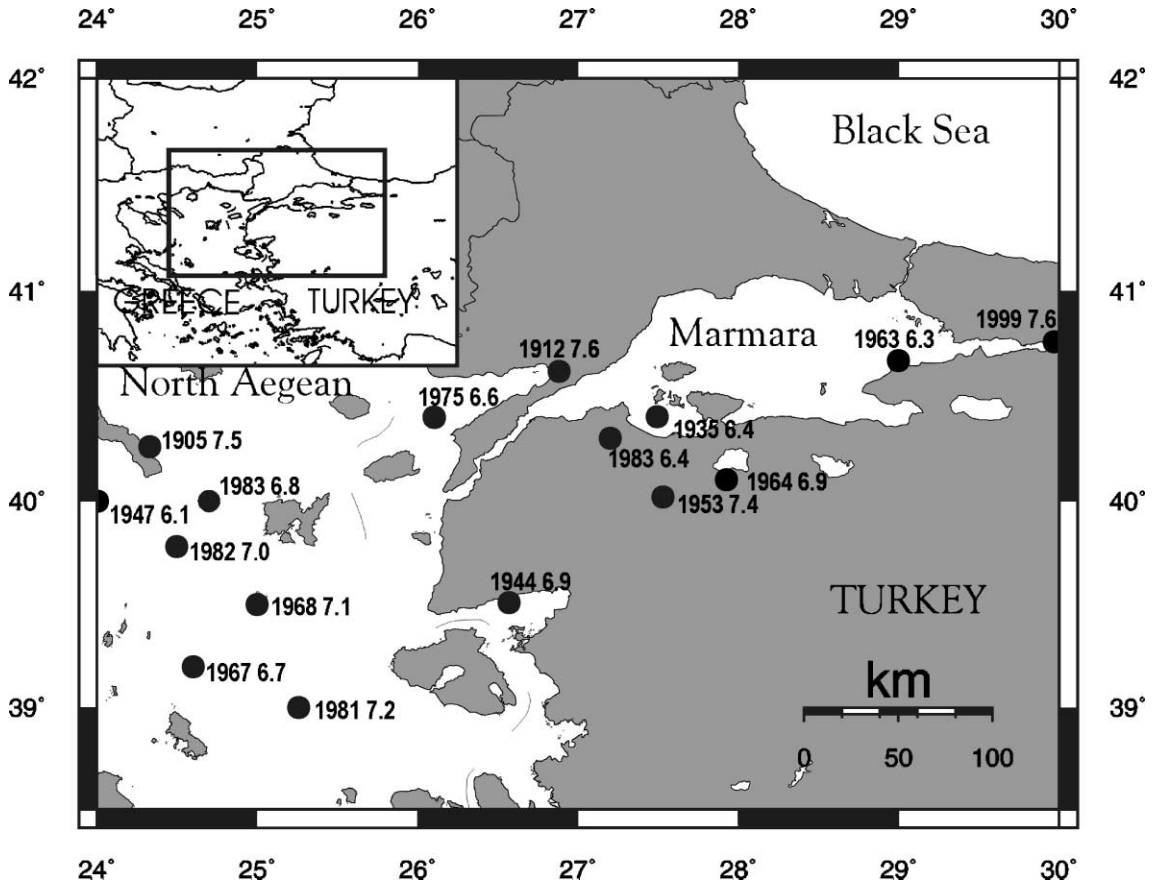

Fig. 1. The investigated area of NW Turkey and North Aegean. The epicenters of all strong ($M \geq 6.0$) mainshocks which occurred in this area during the 20th century are shown.

these papers, estimation of long-term evaluation of seismicity is made on the basis of historical information, studies on stress changes induced by previous earthquakes and GPS measurements of crustal deformation. Some results on the anticipated intermediate-term effects of the Izmit 1999 earthquake on the seismicity of the Aegean area have also been published (Papazachos et al., 2000a).

The purpose of the present work is to investigate the evolution of the seismic activity in this region during the next few years by the application of a recently developed methodology concerning accelerating seismic deformation before strong mainshocks and, in particular, to make a specific prediction of the evolution of this activity.

Accelerating intermediate magnitude seismicity before large earthquakes in relatively broad regions has been observed during the last four decades (Tocher, 1959; Mogi, 1969; Sykes and Jaume, 1990; Knopoff et al., 1996; Jaume and Sykes, 1996, 1999), while studies on cellular automaton models indicate that the largest events tend to be preceded by a power law increase in seismicity associated with a clustering of intermediate-sized events (Huang et al., 1998; Sammis and Smith, 1999).

This work has been intensified during the last decade. It has been shown that the time variation of measures of seismic deformation (seismic moment, Benioff strain, etc.) follows a power law predicted by Statistical Physics, if we consider the process of generation of these moderate magnitude shocks (preshocks) as a critical phenomenon and the large earthquake (mainshock) as a critical point (Sornette and Sornette, 1990; Allegre and Le Mouel, 1994; Ander-

sen et al., 1997). This power law is usually expressed by the following relation proposed by Bufe and Varnes (1993):

$$S(t) = A + B(t_c - t)^m \quad (1)$$

where t_c is the origin time of the mainshock, t is the time before this shock, A, B, m are parameters and $S(t)$ is the cumulative Benioff strain, which is used as a measure of seismic deformation (or of seismicity) and can be calculated by the relation:

$$S(t) = \sum_{i=1}^{n(t)} E_i(t)^{1/2} \quad (2)$$

where E_i is the seismic energy of the ith preshock and $n(t)$ is the number of events which have occurred up to time t. The seismic energy is easily calculated from the moment magnitude of the shocks.

Relation (1) has already been used in some attempts to predict the time and magnitude of several mainshocks (Varnes, 1989; Bufe et al., 1994; Sornette and Sammis, 1995). These attempts, however, have not been based on a systematic way of identifying preshock (critical) regions. A step toward this goal has been made by Bowman et al. (1998) who applied a procedure to identify circular regions approaching criticality before mainshocks of $M \geq 6.5$, which occurred mainly along the San Andreas fault system since 1950, by minimizing a curvature parameter, C, which quantifies the degree of acceleration of the Benioff strain. They defined this parameter as the ratio of the root mean square error of the power law fit (relation (1)) to the corresponding linear fit error.

Observations on accelerating seismicity in the broader Aegean area have been made by several seismologists (Papadopoulos, 1986; Karakaisis et al., 1991; Tzanis et al., 2000). A systematic work on this problem has been carried out during the last 3 years, by using data from this area, which led to the definition of several important properties of the critical earthquake model and to the development of a method for earthquake prediction which is based on this model and on observations of preshock accelerating seismic deformation (Papazachos and Papazachos, 2000a,b; 2001). In the following, this method is briefly presented and is then applied in order to examine the evolution of the intermediate magnitude seismicity in this region.

2. Method and data

The method applied in this paper to predict the epicenter, magnitude and occurrence time of an earthquake is based on the critical earthquake concept (Sornette and Sornette, 1990), on the time-to-failure power law (Bufe and Varnes, 1993) expressed by relation (1), on the quantification of the accelerating deformation by the curvature parameter (Bowman et al., 1998) and on several properties of this model which are expressed by appropriate relations. These relations are the results of an extensive research on accelerated deformation before strong earthquakes ($M \geq 6.0$) which occurred in the broader Aegean area since 1948 and are described in detail in the following.

Papazachos and Papazachos (2000a) considered elliptical areas around the epicenters of several of these strong earthquakes instead of circular ones used by Bowman et al. (1998). After fitting the cumulative Benioff strain released by the preshocks within each ellipse by the power law and the linear model, they calculated the curvature parameter C for various combinations of the geometrical features of the ellipses (length of the major ellipse axis, its azimuth and ellipticity) and different durations of the preshock period. They found that the magnitude of the ensuing mainshock, M, is correlated to the radius, R (in km), of the circle with area equal to the elliptical region, through the relation:

$$\log R = 0.41M - 0.64 \quad \sigma = 0.05. \quad (3)$$

They also found that the duration of the preshock period, t_p (in years) is inversely related to the seismicity of the area, s_r (mean Benioff strain rate in $J^{1/2}$/year/10^4 km^2 calculated from all shocks with $M \geq 5.2$ during the whole instrumental period 1911–1999):

$$\log t_p = 5.81 - 0.75 \log s_r \quad \sigma = 0.17. \quad (4)$$

In subsequent works, Papazachos and Papazachos (2000b, 2001) used data from 52 cases of mainshocks in the Aegean area which were preceded by accelerated seismicity, in order to define relations between the mainshock magnitude M and the parameter B of

relation (1), as well as between M and the mean magnitude, M_{13}, of the three largest preshocks:

$$\log B = 0.64M + 3.27 \quad \sigma = 0.16 \tag{5}$$

$$M = 0.85M_{13} + 1.52 \quad \sigma = 0.21. \tag{6}$$

Parameter A of relation (1), which is the total cumulative Benioff strain including the strain of the mainshock, can be given as the product of the long-term Benioff strain rate S_r (in $J^{1/2}$/year) in the whole preshock critical region and the duration t_p of the preshock activity:

$$A = S_r t_p. \tag{7}$$

Experience gained through the study of the cases mentioned above showed that the initial values of the parameter m of relation (1) and of the curvature parameter C must be smaller than 0.7, since for higher values of these parameters the accelerating behavior of the seismicity expressed in terms of the cumulative Benioff strain is rather weak and practically indistinguishable from a linear time variation. Hence:

$$m < 0.7, \quad C < 0.7. \tag{8}$$

To quantify the compatibility of the values of the parameters R, t_p, B, M, and A calculated for a preshock sequence of an expected mainshock with those determined by relations (3)–(7), which have been derived through the study of the past preshock sequences mentioned above, a parameter P was defined (Papazachos and Papazachos, 2001). This parameter is the average value of the probabilities that each of these five parameters attains a value close to its expected one from these relations, assuming that the deviations of each parameter follow a Gaussian distribution. For example, for the equivalent radius, R, the quantity $Z_R = (\log R - \overline{\log R})/\sigma_{\log R}$ is used ($\overline{\log R}$ is given by relation (3)) as the normalized variable and the corresponding Gaussian probability $P_{\log R}$=erf(Z_R) was determined, with erf() being the error function.

Moreover, a quality index $q(=P/Cm)$ has been suggested (Papazachos et al., 2001a) which incorporates all the constraints posed by relations (3)–(7) on the behavior of the accelerated seismic activity in an area, in order this activity to be considered as a preshock sequence that may lead to the generation of a mainshock. This index reaches its peak value at that geographical point which is the center of the elliptical region that corresponds to the best solution: high P value means that the calculated parameters R, t_p, B, M, and A have values close to the expected ones from relations (3)–(7), whereas low C value indicates strong deviation of the cumulative Benioff strain from the linear behavior and low m value expresses the degree of this non-linear behavior. To sum up: the study of all the cases of past strong mainshocks in the Aegean area showed that in elliptical regions with centers the epicenters of these mainshocks (or close to them), the following cut-off values hold:

$$C \leq 0.60, \quad m \leq 0.35, \quad P \geq 0.45, \quad q \geq 3.0 \tag{9}$$

while their average values and the corresponding standard deviations are:

$$\overline{C} = 0.44 \pm 0.12, \quad \overline{m} = 0.29 \pm 0.06,$$
$$\overline{P} = 0.53 \pm 0.07, \quad \overline{q} = 4.9 \pm 2.1.$$

Accelerating deformation which follows all relations mentioned above cannot be identified (in accordance with the constraints of relation (8)) till a time, t_i (identification time), when this phenomenon is more pronounced due to a precursory seismic excitation that occurs within the preshock region at a time correlated to the mainshock origin time (Papazachos et al., 2001b). The difference $\Delta t_{ci}=t_c-t_i$ between the identification time and the origin time of the mainshock is of the order of several years (3.6 ± 1.6 years) and is given by the relation:

$$\log(t_c - t_i) = 5.04 - 0.75 \log s_r \quad \sigma = 0.18. \tag{10}$$

The curvature parameter C is large (>0.60) at the identification time and gradually decreases as the origin time of the mainshock is approached. The time difference between the origin time of the mainshock and the identification time, deduced from relations (4) and (10), is about 17% of the duration of the preshock sequence. That is:

$$t_c - t_i = (0.17 \pm 0.05) t_p. \tag{11}$$

It is worth mentioning that Yang et al. (2001) independently found that only in the final 1/6 ($\sim$17%) of

the preshock time period can the preshock region be identified. Relations (10) and (11) can be used for estimating the origin time of the oncoming mainshock if the identification time is known. It must be noted that s_r and t_p are estimated by the available data at the identification time.

To apply this method, a grid of points 0.25° apart is defined for the examined area and an algorithm

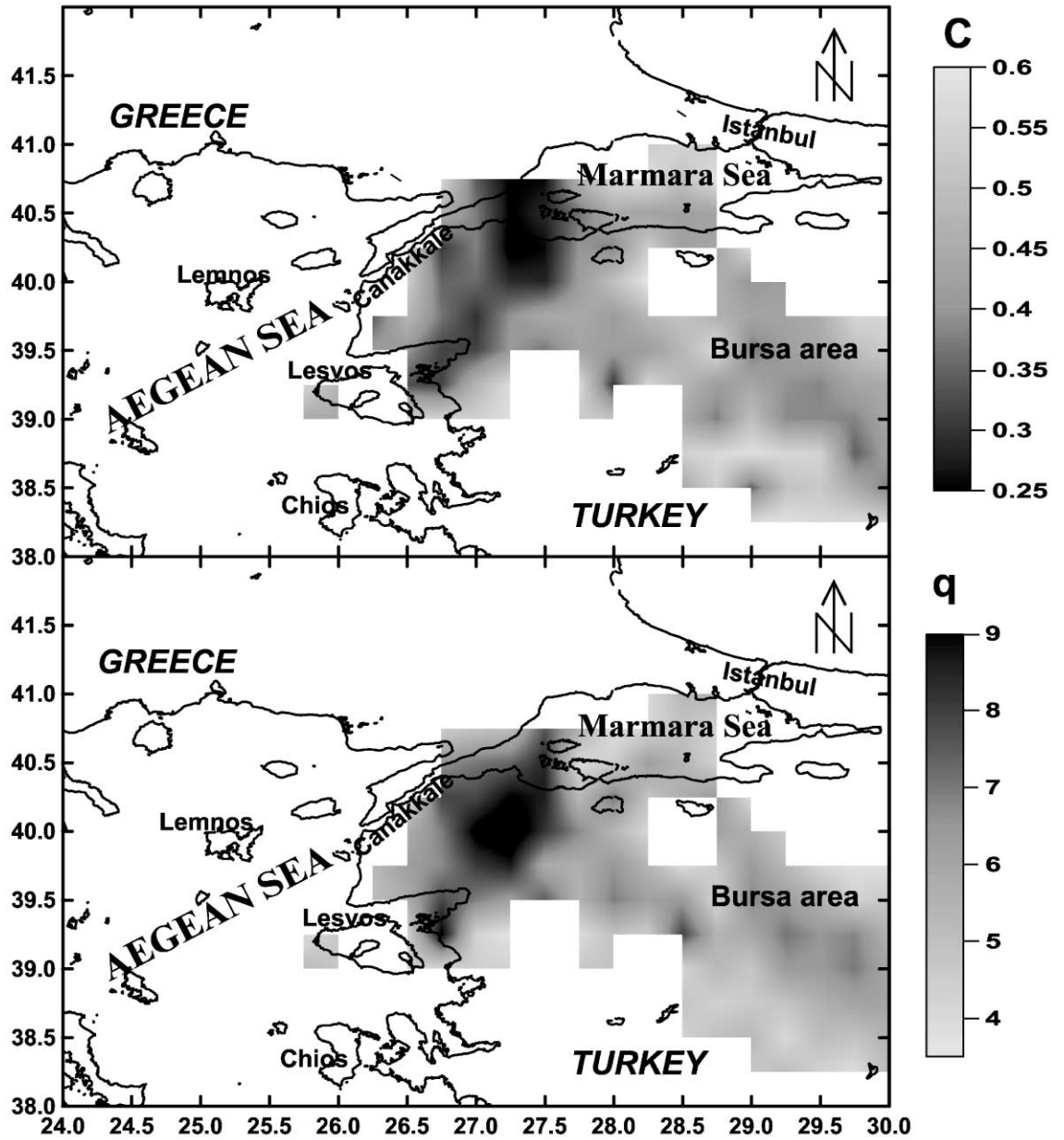

Fig. 2. The spatial distribution of the curvature parameter C (upper) and the quality index q (lower). Dark grey tones correspond to grid points for which local best solutions have been found, whereas blank areas correspond to grid points where the respective solutions are found to be outside the limits of relation (9).

developed by Papazachos (2001) is used for each point to identify regions of accelerating seismic deformation (Benioff strain). According to this algorithm, shocks (preshocks) with epicenters in an elliptical region centered at a certain point of the grid are considered and values for the parameters of relation (1) as well as the curvature parameter C are calculated. Calculations are repeated for several values of the azimuth, z, of the large ellipse axis, of the length, a, of this axis, of the ellipticity, e, and of the time, t_s ($=t_c-t_p$), since when accelerating seismic deformation started. These calculations are also repeated for several magnitudes (typically ranging between M_{min}=5.8 and the magnitude of the largest known earthquake in the area, M_{max}), and for several assumed values of the origin time, t_c, of the mainshock and solutions which fulfill relation (9) are kept. From these solutions, we choose as the "local" best solution the solution with the highest q value. Then, the procedure is repeated for other points of the grid. After examining all the solutions obtained for all the grid points, we calculate the geometrical mean of these solutions (which satisfy relation (9)) and this point is considered as the epicenter of the oncoming mainshock. From all solutions which ful- fill relation (9) the one for which q has the highest value is considered as the best solution and the time corresponding to this solution is considered as a tentative value for the origin time of the oncoming

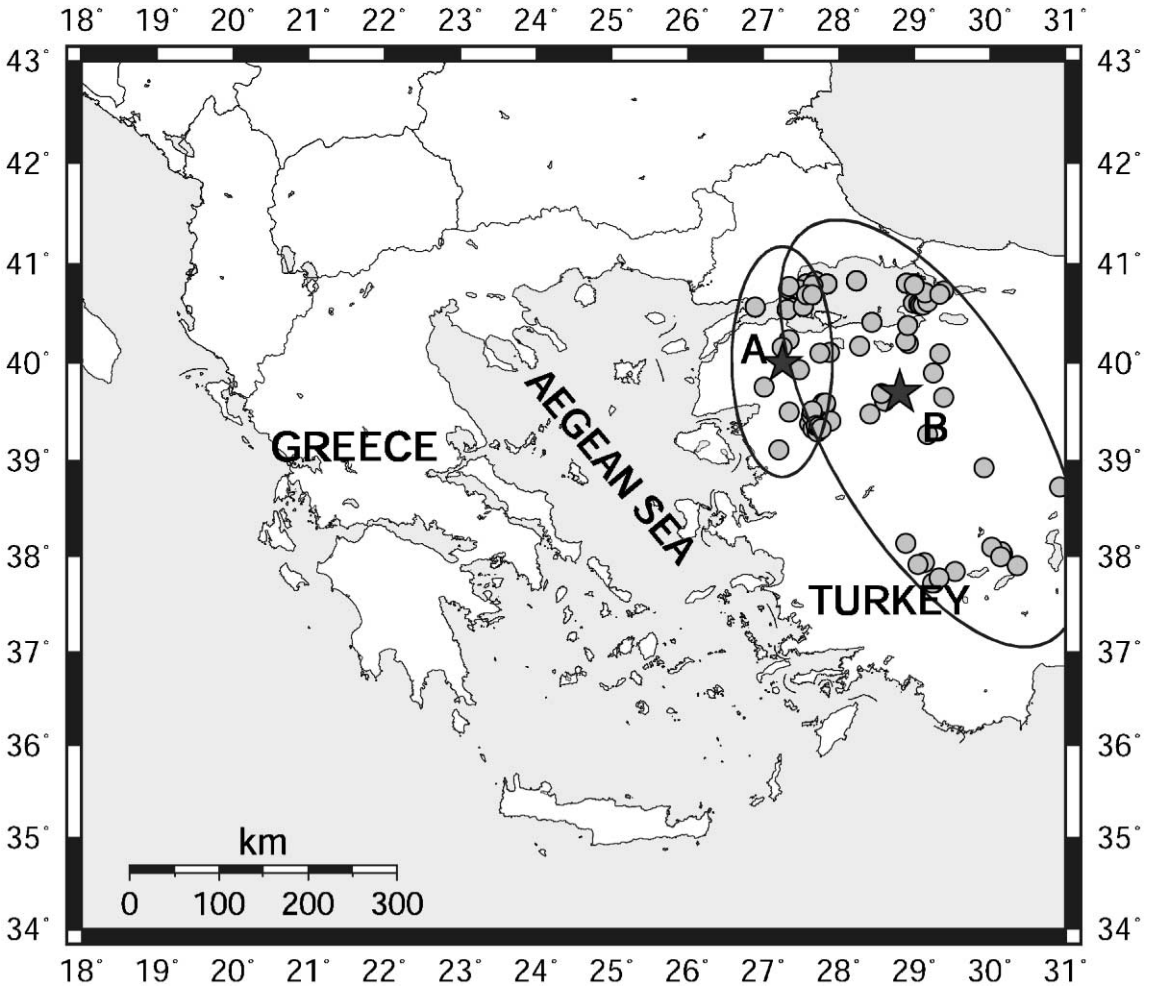

Fig. 3. The elliptical critical regions and the epicenters of preshocks. The stars correspond to the epicenters of the expected mainshocks.

mainshock. The average of the three M values calculated by relations (3), (5), and (6) for the best solution is considered as the magnitude of this mainshock. Using this procedure, the origin time is very roughly estimated because this time is quite sensitive to errors introduced in the performed calculations. For this reason, a second step of calculations is applied, based on an additional technique (see below) that gives a better estimation of the parameters of the expected mainshock and particularly of its origin time.

The technique which is used for a more accurate calculation of the origin time, t_c, of an expected mainshock is based on a change in the relation $T_i=f(T_c)$ between the assumed origin time, T_c, and the calculated identification time, T_i, when T_c becomes equal to t_c (Papazachos et al., 2001b), bearing in mind that the time of observation is always considered as equal to T_i, i.e. the real data used in the calculations concern only preshocks which occur up to the time T_i.

For several assumed origin times, T_c, of the expected mainshock, the corresponding identification times, T_i, are calculated. The change mentioned before is usually an abrupt increase of T_i at $T_c=t_c$. A decrease of C (implying a growing deviation from linearity) is also observed at $T_c=t_c$. This precursory phenomenon gives the possibility for estimating the origin time as well as the identification time, t_i ($T_i=t_i$ at $T_c=t_c$) which can be used in relations (10) and (11) for alternative estimation of t_c. Thus, having a more accurate origin time we repeat the calculation for a more accurate epicenter and magnitude. An example of such a graph is presented later in the text.

It has also been observed (Papazachos et al., 2001b) that this increase of the calculated identification time T_i is associated with strong variations of several relevant parameters: the number, n, of the preshocks increases (seismic excitation), whereas the values of the parameters C, m and t_{13} (difference of the mean origin time of the three largest preshocks and the mainshock origin time) decrease. The increase of the number of preshocks may be attributed to a swarm-like activity (Evison and Rhoades, 1997). On the other hand, C and m decrease since the cumulative Benioff strain exhibits stronger deviation from linearity. The decrease of t_{13} is attributed to the occurrence of at least one of the largest preshocks during this swarm. If we consider the relative rate for each parameter, i.e. the ratio of its rate to the maximum absolute value of the rate observed during the whole period examined, then a measure of the seismic excitation expressed in terms of these five ratios (r_i, r_n, r_c, r_m, r_t) can be calculated for each time interval in which the examined period is separated. Therefore, the average of these five relative values is considered as a measure of this precursory phenomenon and is called Preshock Excitation Indicator (PEI). PEI varies between 0 and 1 in the case of a relative increase of the seismic activity (seismic excitation) with respect

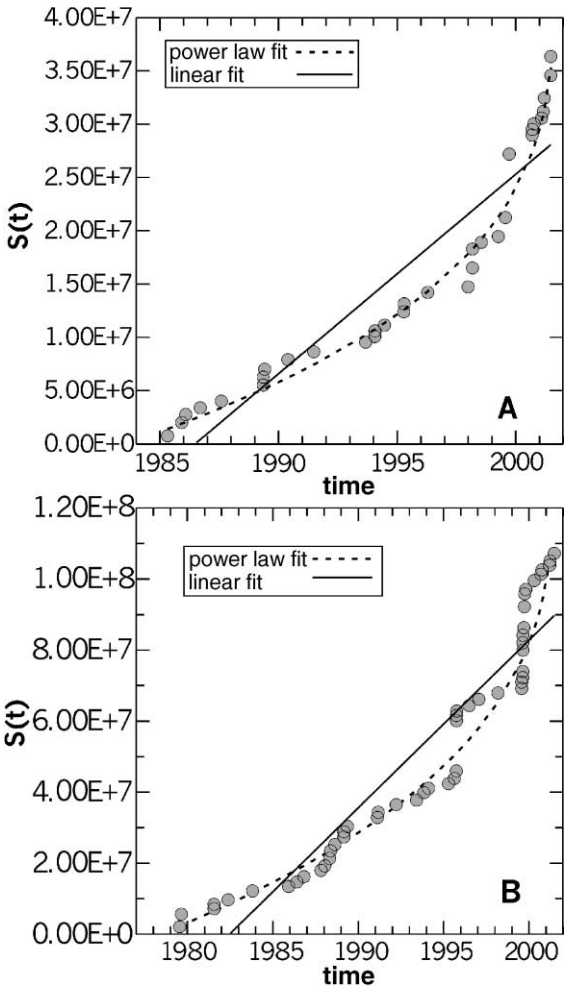

Fig. 4. Time variation of the cumulative Benioff strain, $S(t)$, for the elliptical areas A and B shown in Fig. 3. The dashed curve corresponds to the fit of relation (1), while the solid line to the linear fit.

to the activity predicted by the relation (1) and between −1 and 0 for relative decrease of the seismic activity (seismic quiescence).

The data used to calculate the Benioff strain have been taken from a catalogue compiled by Papazachos et al. (2000b) and belong to one of the following three complete sets of data: 1911–1949 $M \geq 5.2$, 1950–1964 $M \geq 5.0$, 1965–2001 $M \geq 4.5$. The errors in the epicenters are of the order of 15 km for earthquakes which occurred after 1965 (when the first network of seismic stations was established in Greece) and 25 km for older earthquakes. All magnitudes are equivalent moment magnitudes and their errors are up to 0.3. The formula:

$$\log E = 1.5M + 4.7 \quad (12)$$

derived by Papazachos and Papazachos (2000a), has been used to calculate the seismic energy (in Joules) from the moment magnitude and then the Benioff strain is calculated by relation (2).

3. Results

Fig. 2 shows the spatial distribution of the C and q values which have been derived following the previously described approach and satisfy the constraints of relation (9). Blank areas correspond to grid points where the ''local'' best solutions have either C values larger than 0.60 or q values smaller than 3.0. It is observed that most of the smallest values of $C_{\min}$ (<0.4) are distributed in a region which starts from the west Marmara Sea and trends in a SSW direction (dark grey color in Fig. 2). Specifically, there is an area roughly bounded by 26.5°E–27.8°E and 39.2°N–40.7°N where particularly low C and high q values are observed. In this region, the method described in the previous section has been applied to determine the epicenter, the magnitude and the origin time of the expected mainshock as well as the best solution parameters (z, a, e, m, etc.). The best solution in this region, which coincides with the geometrical center of the area where q reaches its largest value, suggests that the expected earthquake will have the following basic focal parameters: M=6.4, t_c=2002.5, φ=40.0°N, λ=27.4°E.

In Fig. 2, another broader area can be identified, where the curvature parameter has also relatively small C and high q values. This area (38.2°N–40.8°N, 28.00°E–30.0°E), which is located east of the already investigated region and has an about NW–SE trend, has also been examined. We found that another strong earthquake can be expected to occur in this area. The epicenter of the expected earthquake is close to that grid point which corresponds to the best solution (highest q value).

Fig. 3 shows the elliptical (preshock) regions which correspond to the best solutions for the expected mainshocks, along with the epicenters of the preshocks. Comparison of Fig. 3 with Fig. 2 shows that the regions of accelerating deformation defined for the expected mainshocks (Fig. 3) have a similar orientation and spatial extent with the areas of very low and relatively low C values, respectively (Fig. 2).

The magnitudes of the preshocks within the elliptical regions were used to calculate the cumulative Benioff strain, $S(t)$, which is shown in Fig. 4 as a function of time. The dashed line is the fit of relation (1) to the data while the solid line corresponds to the linear fit. It is observed that the data are clearly best fitted by the power law model. The examination shows that the region A is at a seismic excitation

Table 1
Parameters of the best solutions of the two expected mainshocks

φ^0_N, λ^0_E	M	t_c	C	m	q	a (km)	z	e	M_{min}	n	t_p	t_s
40.0°N, 27.4°E	6.4	2002.5	0.29	0.22	9.87	130	0°	0.90	4.5	32	17.5	1985
39.2°N, 29.2°E	7.0	2003.5	0.40	0.19	7.18	273	150°	0.90	5.0	50	25.5	1978

The first three columns show the geographic centers of the elliptical regions A and B, the magnitudes, M, of these mainshocks and their origin times, t_c. The values of parameters C, m and q are given in the next six columns along with the geometrical characteristics of the elliptical areas for these solutions (length, a [in km], of the major ellipse axis, its azimuth, z, and ellipticity, e). The last four columns give information on the cut-off magnitudes, M_{min}, of the preshocks considered, their numbers, n, the durations of the preshock period, t_p, and the years, t_s, since when the accelerating preshock deformation started.

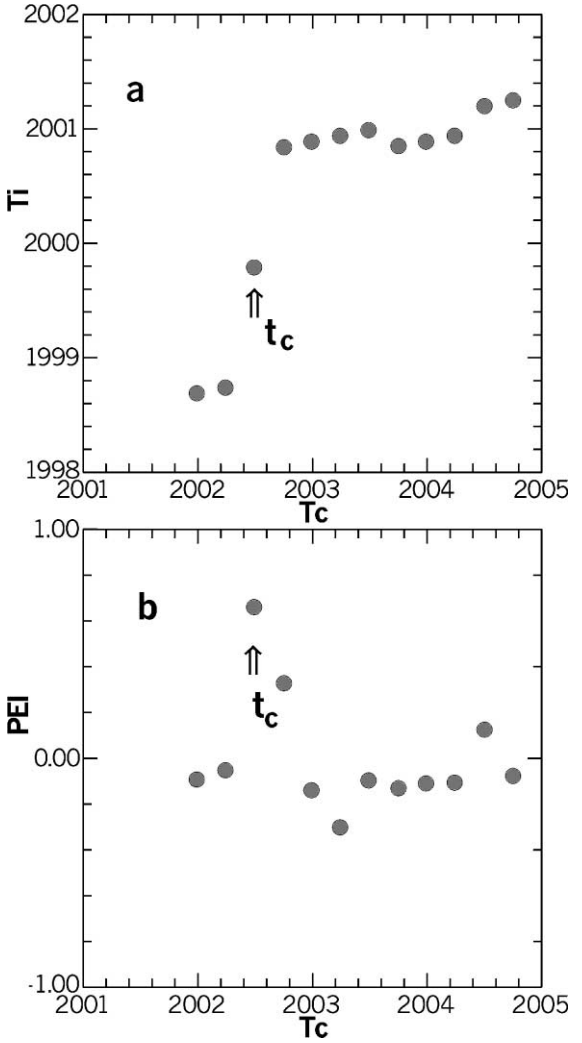

Fig. 5. Variation of the calculated identification time, T_i, (a), and of the Preshock Excitation Indicator (PEI) (b), as a function of the assumed origin time, T_c, for the broader Canakkale region (ellipse A in Fig. 3). An abrupt increase of T_i as well as of PEI is observed at T_c=2002.5 years. The arrows show the predicted origin time, t_c.

(acceleration) since 1985, whereas the preshock activity in region B started in 1978. The excitation in the region B can be a part of the seismic activity which led to the generation of the large Izmit, 1999 earthquake or is a preshock activity which will lead to the generation of a new oncoming mainshock. The resolution of this ambiguity is a difficult problem. It is probable that more data need to be accumulated before we can finally resolve the character of the observed acceleration. If we accept the interpretation that this is a preshock activity of an oncoming mainshock, the following basic focal parameters of this mainshock can be determined: M=7.0, t_c=2003.5, φ=39.7°N, λ=28.8°E.

The complete solution vectors for the best solutions of the two expected strong earthquakes are listed in Table 1. In the first three columns of this table, the

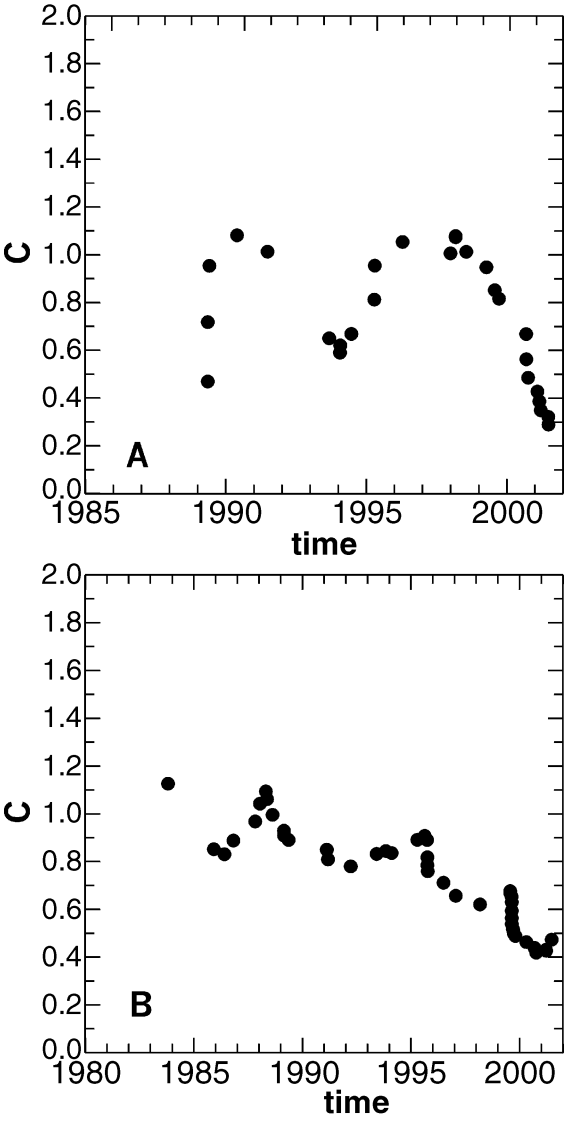

Fig. 6. Time variation of the C value for the two elliptical areas (see text for explanation).

geographic coordinates of the points which correspond to the best solutions (φ_N°, λ_E°), the magnitude, M, and the origin time t_c are given. In the same table the other parameters of the best solutions are given. These are the curvature parameter, C, the parameter, m, the quality index, q, the length of the large ellipse axis, a (in km), its azimuth, z, and the ellipticity, e. The minimum magnitude for the preshocks, M_{min}, the number of observations, n (number of preshocks plus the mainshock), the duration, t_p, of the preshock sequence and the year, t_s, since when the accelerating preshock deformation started, are also shown.

Fig. 5a shows a plot of the calculated identification time, T_i, as a function of the assumed origin time, T_c, for the expected mainshock in the region A and Fig. 5b shows the plot of the Preshock Excitation Indicator (PEI) as a function of T_c. It is clear that at T_c=2002.5, an abrupt increase of the calculated identification time T_i is observed (from 1998.7 to 1999.8), as well as an increase of PEI which reaches its highest value in the whole interval examined, and therefore the origin time of the expected mainshock is t_c=2002.5 according to this method. Similar graphs have been examined for the expected mainshock in the region B.

We have also examined the time variation of the C parameter in the two regions, since it is expected that as we approach the time of the mainshock, the accelerating behavior of the seismic activity is more pronounced. The time variation of the parameter C, calculated without considering the mainshock magni-

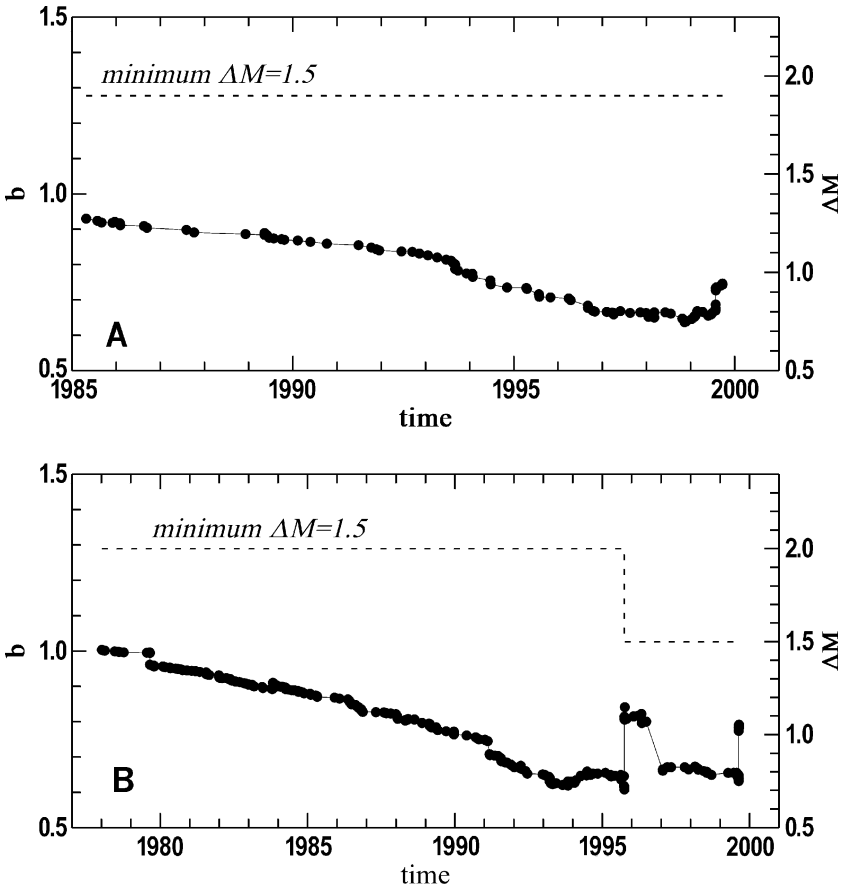

Fig. 7. Time variation of the b values of the Gutenberg–Richter recurrence law for the earthquakes in the ellipses A and B of Fig. 3. A moving window of at least 40 events has been used, while the magnitude range, ΔM, is always larger than or equal to 1.5.

tude, is shown in Fig. 6. The first six preshocks of each critical region were considered and all parameters of relation (1), as well as the curvature parameter C, were calculated. Then, the number of preshocks was increased until the total number of preshocks within the critical region (excluding the mainshock) was reached. It is observed that the C values decrease as the expected mainshock origin time is approached. Such decreasing trend of the C parameter with time has already been observed before past strong earthquakes in the broader Aegean area (Karakaisis et al., 2002a), as well as in several elliptical regions in this area where accelerating seismic activity is currently observed (Papazachos et al., 2001a,c; Karakaisis et al., 2002b).

The systematic increase in intermediate-level seismicity prior to strong earthquakes which has been proposed by several authors (Varnes, 1989; Bufe et al., 1994; Jaume and Sykes, 1999) is also frequently reflected in the frequency–magnitude distribution. For this reason we studied the time variation of the values of the parameter b of the Gutenberg and Richter recurrence law (1944) and we consider not only the preshocks used to determine the Benioff strain in these elliptical areas but all the complete data above a certain cut-off magnitude (4.0 for area A and 4.4 for area B). For each ellipse, we first calculated the b_{ell} value for the whole preshock period. Then, b values were calculated for a moving window of at least 40 events, with a step of one event, under the constraint that the magnitude range was at least 1.5 (Papazachos, 1974). Both constraints (minimum number of 40 events and magnitude range) were used to avoid instabilities in estimating the b values. These b values have been plotted, after division by b_{ell}, against time and are shown in Fig. 7. Decreasing b values can be observed for both cases, in accordance to similar results for several past strong earthquakes in the Aegean area (Karakaisis et al., 2002a).

Regarding the uncertainties of the basic focal parameters of the expected mainshock (epicenter, magnitude, origin time), Papazachos et al. (2001d) estimated such uncertainties by applying the same method to make retrospective predictions for 18 recent strong earthquakes in the broader Aegean area and compared the results with the observed parameters. Based on their results we can conclude that there is a high probability (>90% confidence) for the epicenters of the expected mainshocks to be within a distance of less than 100 km from the given ones. The corresponding uncertainties are ± 0.5 for the magnitude and ± 1.5 years for the origin times of the expected mainshocks.

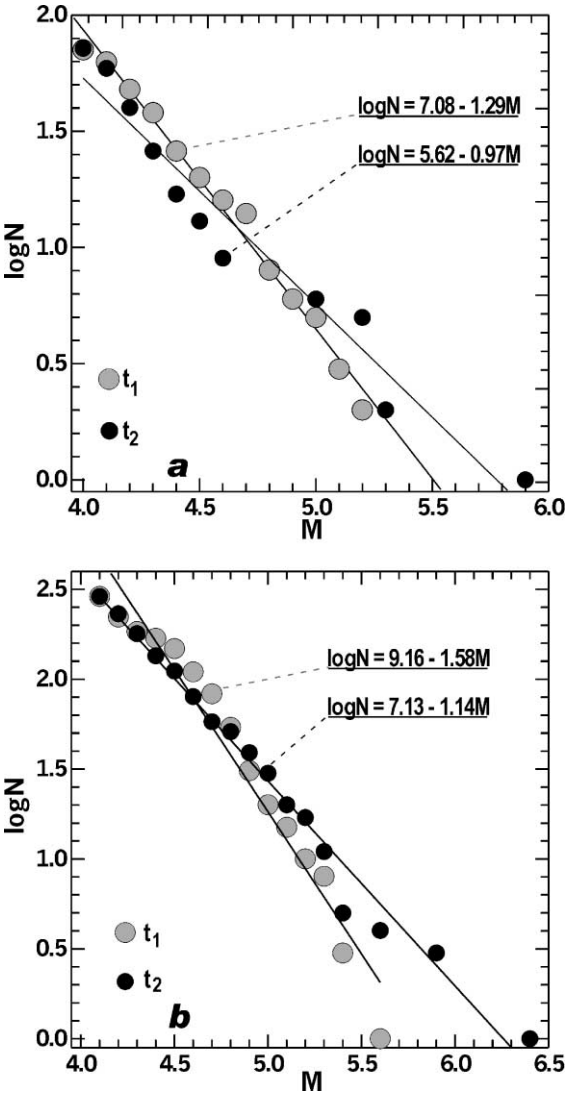

Fig. 8. b values calculated for the first and second halves t_1 and t_2 into which the preshock catalogue of each ellipse (A and B) has been divided. In both cases, it is observed that the b values of the later period (t_2, black circles) are smaller than the corresponding values of the earlier period (t_1, grey circles), in agreement with independent observations in other areas (Jaume and Sykes, 1999).

4. Discussion

It is not yet known whether accelerating seismicity always leads to a mainshock generation, while some cases have been reported in which no clearly distinguishable accelerating seismicity was observed before some mainshocks (Bowman, 1992; Bufe et al., 1994). However, recent relevant work for the Aegean area (Papazachos and Papazachos, 2000a,b, 2001) shows that all recent strong earthquakes for which reliable data are available were preceded by accelerating seismicity. Moreover, the fact that the procedure followed throughout the present work resulted in the identification of an elliptical region in the North Aegean where a strong (M=6.3) shallow earthquake occurred on 26 July 2001, that is, about 10 months after the identification of the region (Karakaisis et al., 2002b), is encouraging.

An additional observational evidence that seismic activation takes place now in the elliptical regions of Fig. 3 is based on the seismic activation hypothesis of Rundle et al. (2000) who suggest that there is an increase in the rate of occurrence of intermediate-sized earthquakes prior to the generation of the mainshock, whereas the rates at which smaller earthquakes occur during a seismic cycle are independent of time. Jaume and Sykes (1999) tested this hypothesis by examining the frequency–magnitude distribution of earthquakes during earlier and later periods of four preshock sequences and found that three of them fitted this hypothesis. We have also tested this hypothesis and for this reason, we split the complete preshock catalogue of each elliptical region into two halves t_1 and t_2 and calculated the respective b values (Fig. 8). In both cases we found that the b values of the second half (black circles), which correspond to the later periods of the preshock activity, are considerably smaller than the b values of the first halves (grey circles) that correspond to the earlier periods.

We can therefore conclude that the currently observed accelerating seismic crustal deformation (Benioff strain) in the westernmost part of North Anatolian Fault Zone will very probably culminate by the generation of at least one strong (M>6.0) mainshock during the next few years. Simple calculations show that the probability of occurrence of a main event within the specified space–time–magnitude range by random chance is about 9% for the elliptical region (ellipse A) of Canakkale and 2% for the elliptical region of Bursa (ellipse B).

The results presented in this study show that the epicenter of the probably ensuing earthquake (40.0°N, 27.4°E) in the broader Canakkale region, as well as the epicenter (39.7°N, 28.8°E) of the probably ensuing mainshock in the broader eastern Marmara area, are located in the southern branch of the western part of the North Anatolian Fault Zone (see Fig. 2). This observation probably indicates that this branch will be activated during the next few years. Independently of the occurrence or not of these mainshocks, the accelerating seismic deformation in this area (manifested by the generation of intermediated magnitude shocks) is an observational fact (see Fig. 4). Some of these shocks may be strong enough ($M \sim 6.0$) and capable of producing damage in this densely populated area.

Acknowledgements

The paper benefited significantly from the comments and suggestions of P. Suhadolc and S. Jaume, to whom we express our thanks. Thanks are also due to Wessel and Smith (1995) for their generous distribution of the GMT software used to generate most of the maps of this study. This work has been partially supported by the Greek Planning and Protection Organization (OASP) (Res. Comm. AUTH project 20242) and is a Geophysical Laboratory contribution number 0556/2001.

References

Allegre, C.J., Le Mouel, J.L., 1994. Introduction of scaling techniques in brittle failure of rocks. Phys. Earth Planet. Inter. 87, 85–93.

Allen, C., 1969. Active faulting in northern Turkey. Contr. No. 1577., Div. Geol. Sci. Calif. Inst. Tech., 2.

Ambraseys, N.N., Finkel, C.F., 1995. The Seismicity of Turkey, Eren Press, Istanbul.

Ambraseys, N.N., Jackson, J.A., 2000. Seismicity of the Sea of Marmara (Turkey) since 1500. Geophys. J. Int. 141, F1–F6.

Andersen, J.V., Sornette, D., Leung, K.T., 1997. Tri-critical behavior in rupture induced by disorder. Phys. Rev. Lett. 78, 2140–2143.

Bowman, J.R., 1992. The 1988 Tennant Creek, Northern Territory, earthquakes: a synthesis. Aust. J. Earth Sci. 39, 651–699.

Bowman, D.D., Ouillon, G., Sammis, C.G., Sornette, A., Sornette,

D., 1998. An observational test of the critical earthquake concept. J. Geophys. Res. 103, 24359–24372.

Bufe, C.G., Varnes, D.J., 1993. Predictive modelling of seismic cycle of the Great San Francisco Bay Region. J. Geophys. Res. 98, 9871–9883.

Bufe, D.G., Nishenko, S.P., Varnes, D.J., 1994. Seismicity trends and potential for large earthquakes in the Alaska–Aleutian region. Pure Appl. Geophys. 142, 83–99.

Dewey, J.W., 1976. Seismicity of northern Anatolia. Bull. Seismol. Soc. Am. 66, 843–868.

Evison, F.F., Rhoades, D.A., 1997. The precursory earthquake swarm in New Zealand. N. Z. J. Geol. Geophys. 40, 537–547.

Gutenberg, B., Richter, C.F., 1944. Frequency of earthquakes in California. Bull. Seismol. Soc. Am. 34, 185–188.

Huang, Y., Saleur, H., Sammis, C., Sornette, D., 1998. Precursors, aftershocks, criticality and self organized criticality. Europhys. Lett. 41, 43–48.

Hubert-Ferrari, A., Barka, A., Jacques, E., Nalbant, S.S., Meyer, B., Armijo, R., Tapponier, P., King, G.C.P., 2000. Seismic hazard in the Marmara sea region following the 17 August 1999 Izmit earthquake. Nature 404, 269–273.

Jaume, S.C., Sykes, L.R., 1996. Evolution of moderate seismicity in the San Francisco Bay region, 1850 to 1993: seismicity changes related to the occurrence of large and great earthquakes. J. Geophys. Res. 101, 765–789.

Jaume, S.C., Sykes, L.R., 1999. Evolving towards a critical point: a review of accelerating seismic moment/energy release rate prior to large and great earthquakes. Pure Appl. Geophys. 155, 279–306.

Karakaisis, G.F., Kourouzidis, M.C., Papazachos, B.C., 1991. Behavior of the seismic activity during a single seismic cycle. International Conference on Earthquake prediction: State-of-the-art, Strasbourg, France, 15–18 October, 47–54.

Karakaisis, G.F., Savvaidis, A.S., Papazachos, C.B., 2002a. Time variation of parameters related to the accelerating preshock crustal deformation in the Aegean area. Pure Appl. Geophys., in press.

Karakaisis, G.F., Papazachos, C.B., Savvaidis, A.S., Papazachos, B.C., 2002b. Accelerating seismic crustal deformation in the North Aegean Trough, Greece. Geophys. J. Int., in press.

Knopoff, L., Levshina, T., Keilis-Borok, V.J., Mattoni, C., 1996. Increased long-range intermediate-magnitude earthquake activity prior to strong earthquakes in California. J. Geophys. Res. 101, 5779–5796.

Mogi, K., 1969. Some features of the recent seismic activity in and near Japan: 2. Activity before and after great earthquakes. Bull. Earthquake Res. Inst., Univ. Tokyo 47, 395–417.

Papadimitriou, E.E., Karakostas, B.G., Papazachos, B.C., 2001. Rupture zones in the area of 17.08.99 Izmit (NW Turkey) large earthquake (M_w7.4) and stress changes caused by its generation. J. Seismol. 5, 269–276.

Papadopoulos, G.A., 1986. Long term earthquake prediction in western Hellenic arc. Earthquake Pred. Res. 4, 131–137.

Papazachos, B.C., 1974. Dependence of the seismic parameter b on the magnitude range. Pure Appl. Geophys. 112, 1059–1065.

Papazachos, C.B., 2001. An algorithm of intermediate-term earthquake prediction using a model of accelerated seismic deformation. 2nd Hellenic Conf. on Earthquake Engineering and Engineering Seismology, 28–30 November 2001, 10 pp.

Papazachos, B.C., Papazachou, C.B., 1997. The Earthquakes of Greece. Ziti Publications, Thessaloniki, p. 304.

Papazachos, B.C., Papazachos, C.B., 2000a. Accelerated preshock deformation of broad regions in the Aegean area. Pure Appl. Geophys. 157, 1663–1681.

Papazachos, C.B., Papazachos, B.C., 2000b. Observations on preshock seismic deformation in the Aegean area and earthquake prediction. 27th Gen. Assembly Europ. Seismol. Comm., Lisbon, Portugal, 10–15 Sept., 301–305.

Papazachos, C.B., Papazachos, B.C., 2001. Precursory accelerated Benioff strain in the Aegean area. Ann. Geofis. 44, 461–474.

Papazachos, B.C., Karakaisis, G.F., Papazachos, C.B., Scordilis, E.M., 2000a. Triggering of strong earthquakes in the North and East Aegean Plate Boundaries by westward motion of the Anatolia Plate. Geophys. Res. Lett. 27, 3957–3960.

Papazachos, B.C., Comninakis, P.E., Karakaisis, G.F., Karakostas, B.G., Papaioannou, Ch. A., Papazachos, C.B., Scordilis, E.M., 2000b. A catalogue of earthquakes in Greece and surrounding area for the period 550 BC–1999. Publ. Geoph. Lab., Univ. of Thessaloniki (also at http://geohazards.cr.usgs.gov/iaspei/europe/greece/the/catalog.txt).

Papazachos, C.B., Karakaisis, G.F., Savvaidis, A.S., Papazachos, B.C., 2001a. Accelerating seismic crustal deformation in the southern Aegean area. Bull. Seismol. Soc. Am., in press.

Papazachos, B.C., Karakaisis, G.F., Papazachos, C.B., Scordilis, E.M., Savvaidis, A.S., 2001b. A method for estimating the origin time of an ensuing mainshock by observations of preshock seismic crustal deformation. Proc. 9th International Congress Geol. Soc. Greece, 20–25 Sept. 2001, Athens 4, 1573–1579.

Papazachos, B.C., Savvaidis, A.S., Papazachos, C.B., Karakaisis, G.F., 2001c. Precursory seismic crustal deformation in the area of southern Albanides. J. Seismol., in press.

Papazachos, C.B., Karakaisis, G.F., Scordilis, E.M., 2001d. Results of a retrospective prediction of past strong mainshocks in the broader Aegean area by application of the accelerating seismic deformation method. Pure Appl. Geophys., submitted for publication.

Parsons, T., Toda, S., Stein, R.S., Barka, A., Dieterich, J.H., 2000. Heightened odds of large earthquakes near Istanbul: an interaction-based probability calculation. Science 288, 661–665.

Rundle, J.B., Klein, W., Turcotte, D.L., Malamud, B.D., 2000. Precursory seismic activation and critical-point phenomena. Pure Appl. Geophys. 157, 2165–2182.

Sammis, C.G., Smith, S.W., 1999. Seismic cycles and the evolution of stress correlation in cellular automaton models of finite fault networks. Pure Appl. Geophys. 155, 307–334.

Sornette, A., Sornette, D., 1990. Earthquake rupture as a critical point. Consequences for telluric precursors. Tectonophysics 179, 327–334.

Sormette, D., Sammis, C.G., 1995. Complex critical exponents from renormalization group theory of earthquakes: implications for earthquake predictions. J. Phys. I (France) 5, 607–619.

Stein, R.S., Barka, A.A., Dieterich, J.H., 1997. Progressive failure on the North Anatolian fault since 1939 by earthquake stress triggering. Geophys. J. Int. 128, 594–604.

Sykes, L.R., Jaume, S., 1990. Seismic activity on neighboring faults as a long term precursor to large earthquakes in the San Francisco Bay area. Nature 348, 595–599.

Tocher, D., 1959. Seismic history of the San Francisco bay region. Calif. Div. Mines Spec. Rep. 57, 39–48.

Toksoz, M.N., Shakal, A.F., Michael, A.J., 1979. Space–time migration of earthquakes along the north Anatolian fault zone and seismic gaps. Pure Appl. Geophys. 117, 1258–1270.

Tzanis, A., Vallianatos, F., Makropoulos, K., 2000. Seismic and electric precursors to the 17-1-1983, M7 Kefallinia earthquake, Greece: signatures of a SOC system. Phys. Chem. Earth 25, 281–287.

Varnes, D.J., 1989. Predicting earthquakes by analyzing accelerating precursory seismic activity. Pure Appl. Geophys. 130, 661–686.

Wessel, P., Smith, W., 1995. New version of the Generic Mapping Tools, EOS. Trans. Am. Geophys. Union 76, 329.

Yang, W., Vere-Jones, D., Li, M., 2001. A proposed method for locating the critical region of a future earthquake using the critical earthquake concept. J. Geophys. Res. 106, 4121–4128.